MECHANICAL TESTING AND EVALUATION OF EPOXY RESINS AT CRYOGENIC TEMPERATURES

By

Justin Reed Jackson

A Thesis
Submitted to the Faculty of
Mississippi State University
in Partial Fulfillment of the Requirements
for the Degree of Masters of Science
in Mechanical Engineering
in the Department of Mechanical Engineering

Mississippi State, Mississippi

December 2005

MECHANICAL TESTING AND EVALUATION OF EPOXY RESINS AT CRYOGENIC TEMPERATURES

By

Justin Reed Jackson

Approved:

Judy Schneider Associate Professor of Mechanical Engineering (Director of Thesis)	Richard Patton Assistant Professor of Mechanical Engineering (Committee Member)
Anthony J. Vizzini Professor and Head of Aerospace Engineering Department (Committee Member)	Steve Daniewicz Professor and Graduate Coordinator of Mechanical Engineering Department

Roger King
Associate Dean
Bagley College of Engineering

Name: Justin Reed Jackson

Date of Degree: December 09, 2005

Institution: Mississippi State University

Major Field: Mechanical Engineering

Major Professor: Dr. Judy Schneider

Title of Study: MECHANICAL TESTING AND EVALUATION OF EPOXY RESINS AT CRYOGENIC TEMPERATURES

Pages in Study: 50

Candidate for Degree of Masters of Science

The objective of this research is to develop a test methodology to be used in determining which material properties affect the ultimate performance of a composite overwrapped pressure vessel (COPV) at liquid nitrogen (LN_2) temperatures. The test methodology being evaluated is based on that used for ambient performance of COPVs and includes: resin properties, resin/fiber interface and COPV burst data. The resin properties are investigated by use of tensile tests to determine: strain to failure (%ε), failure stress (σ_{ys}), and elastic modulus (E). The resin/fiber interface is evaluated using short beam shear tests to determine the interlaminar shear strength (ILSS). These properties are compared with actual COPV burst pressures performed at ambient and LN_2 temperatures. If a correlation can be found, this research lays the foundation for a method to quickly and efficiently screen candidate material systems for composite overwrapped pressure vessel (COPV) fabrication.

DEDICATION

I would like to partially dedicate this work to my parents, Sonja and Roger Jackson. Without their financial and emotional support this work would not have been possible. Also, to Ms. Kristen Cameron, its been a long ride but its finally over.

"*You are no longer to supply the people with straw for making bricks; let them go and gather their own straw"*-**Exodus 5.7**

ACKNOWLEDGMENTS

The author expresses his sincere gratitude to the many people without whose assistance and guidance this thesis could not have been completed. First and foremost, to my major professor, Dr. Judy Schneider, thank you for your patience and guidance throughout this research project and thesis process. Sincere thanks are due to my thesis committee members especially Dr. Anthony Vizzini for the priceless consulting. Also the author would like to acknowledge the unparalled support from NASA Marshall, thanks to Mr. Tom Delay, Mrs. Mindy Niedermeyer, and Dr. Alan Nettles. I would like to acknowledge the funding provide by NCAM Grant #58404-511, under the management of Bruce Brailsfort at UNO and John Vickers at NASA-MSFC

TABLE OF CONTENTS

LIST OF TABLES

LIST OF FIGURES

FIGURE Page

CHAPTER I

INTRODUCTION

Throughout the history of space flight, cryogenic propellants have been used to power launch vehicles. The initial use of liquid oxygen (LOX) as an oxidizer in a bi-propellant system dates back to 1926, when Robert H. Goodard tested the first liquid propellant rocket engine. During the 1960's liquid oxygen was combined with liquid hydrogen to create the first high energy rocket propellant and was used in the upper stage of the Saturn V rocket [1].

Traditionally aluminum has been used for the fabrication of cryogenic fuel tanks. Aluminum, which has a face centered cubic (FCC) crystalline structure, does not encounter embrittlement problems at low temperatures like body centered cubic (BCC) crystalline structured metals. In addition, the low density of aluminum (2.7 g/cc) is favorable for reducing the weight of the fuel tank in high strength driven applications. Since the 1960's, the design of rocket engines has been moving to higher-pressure regions. To meet the higher strength to weight requirements, the use of polymeric composite systems is being pursued.

The rapid development of polymer composite technology is exceeding the advancement of polymer composite science. Most of the development work in this area

is done by either private industry or defense related and hence proprietary. Many industries are working toward the goal of developing a polymer resin to operate favorably in the cryogenic regions. However, when coupled with the various fibers available and design philosophies, this leads to a large number of combinations for evaluation. Thus the need has arisen for a quick and inexpensive screening method to identify promising polymer resins for use at cryogenic temperatures. There is little published literature on correlating material properties to actual tank performance. Garrett[2] investigated the effect of resin failure strain on the tensile properties of glass fiber reinforced polyester cross ply laminates. Lu [3] and Cohen [4] investigated the influence of resin properties and the strength of filamentary structures. Lu [3] concluded that the strength of a composite overwrapped pressure vessels was related to the interlaminar shear strength (ILSS) of the composite material. Cohen [4] concluded that delivered fiber strength variability of filamentary structures can be contributed to the neat resin properties, specifically fracture toughness, elongation at yield (ε_{ys}), and initial modulus (E) and the yield strength (σ_{ys}). However, all of this work was done at ambient temperatures and may not be applicable with the composite overwrapped pressure vessel (COPV) performance below its glass transition temperature (T_g). Although the actual operating environment of the high-pressure vessels for aerospace applications will be for storage of liquid hydrogen (10K) and liquid oxygen (90K), evaluation tests are run using liquid nitrogen (77K) to minimize the flammability damage.

The applications for carbon fiber reinforced polymer (CFRP) composite structures and COPVs are increasing. In the near future, light-weight, high-strength vessels that

operate at low temperatures will be considered for applications ranging from space exploration to transportation of natural gas. CFRPs and COPVs offer an attractive alternative high strength to weight ratio material to conventional all metal pressure vessels. Because these applications require the composite polymer matrix to operate well below T_g, it is imperative to understand the mechanical properties of polymer resin systems at cryogenic temperatures.

This research project will be concerned with developing a test methodology and material property data base to characterize candidate neat resin systems at low temperatures. The screening tests developed for this study were based on room temperature standards and modified slightly for use at LN_2 temperatures. The properties of neat polymer resins are investigated by use of tensile tests to determine the strain to failure of the resin ($\%\varepsilon_f$), yield strength (σ_{ys}) and elastic modulus (E). Evaluations of the fiber-matrix interaction were conducted using the short beam shear test to determine the interlaminar shear strength (ILSS) [3]. Finally 7.5 liter COPVs were fabricated with the candidate resin systems and subjected to liquid nitrogen burst tests. The 7.5 liter tanks were fabricated and tested by the NASA-Marshall Space Flight Center. The processing variables were held constant and a Toray M30SC carbon fiber was used. All tests were conducted with the test article completely submerged in LN_2 to insure a constant temperature, and the tests were performed at a constant rate so a valid comparison could be made.

Chapter II will give the reader an overview of the basic filament winding process as well as current composite overwrapped pressure vessels technology. Chapter III

discusses the various types of microstructure encountered with polymers. The goal of this chapter is to illustrate that the microstructure plays an important role in the behavior of the polymer. Chapter III also discusses the response of polymers at low temperatures and how behavior of the microstructure changes. Chapter IV focuses on the experimental steps that were taken to evaluate the neat resin properties and the ILSS as determined by the short beam shear test. Chapter V presents the results form the various tests and Chapter VI discusses these results.

CHAPTER II

COMPOSITE PRESSURE VESSEL TECHNOLOGY

Liquid propellants such as liquid hydrogen and liquid oxygen were initially stored in insulated aluminum alloy tanks. Current metallic tank technology has not significantly changed. The use of metal tanks creates a weight issue that limits the payload and range of launch vehicles [5]. Utilizing polymer composite materials can facilitate this weight issue. Carbon fiber reinforced polymer cryogenic propellant fuel tanks, with an average density of 1.5 g/cc, can be used to reduce the weight issue associated with an all aluminum tank, with an average density of 2.7 g/cc. In the filament winding process, continuous tapes, or plies, of polymer-impregnated fibers are wrapped over a rotating mandrel to form an axisymmetric part.

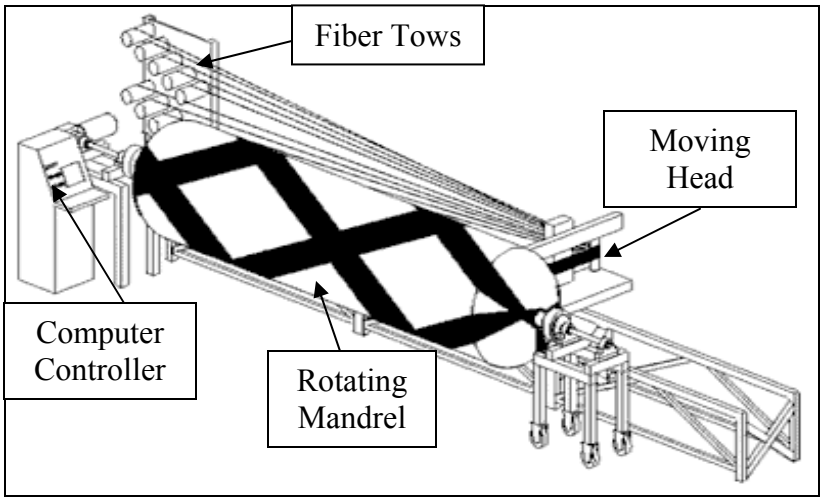

Figure 2.1 basic filament winding process [6]

1. Composite overwrapped pressure vessel fabrication

Figure 2.1 illustrates the basic filament winding process for fabrication of composite overwrapped pressure vessels (COPV). The continuous fibers are pulled from creels through a resin bath. Fiber tension is controlled by force feed back system located before the resin bath. Once the fiber bundles or rovings have been impregnated with resin they undergo a wiping process designed to remove excess resin. The wiped rovings are gathered together to form the flat band that is positioned on the mandrel. Successive layers, or plies, are added at the same or different winding, or wind-angles, until the required thickness is reached and the part is subsequently cured by autoclaving or an elevated oven cure [7]. The filament winding process described produces a helical winding pattern illustrated in Figure 2.2.

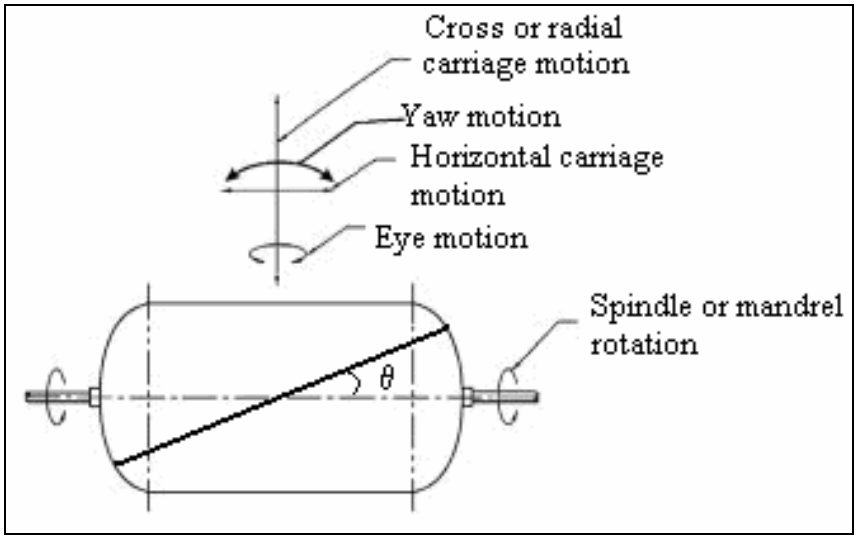

Figure 2.2 helical winding of COPV [8]

The orientation of the band with respect to the axis of the mandrel is called the wind angle. By adjusting the mandrel rotational speed and carriage travel speed, any wind angle can be obtained between near 0° to near 90°. Because the mandrel is rotating and the carriage is moving along the axis of the mandrel true 0° or 90° wind angles cannot be reached. However, the movement of the feed carriage causes the fiber bands to crisscross at plus and minus the wind angle. The crisscrossing causes a weaving effect and the layers can be considered as a single orthotropic laminae [9].

The important process parameters in the filament winding process are fiber tension, fiber wet-out, and resin content [8]. Fiber tension is important in the manufacturing of reliable parts because it affects both resin content and void content. The fiber tension controls the pressure on the layers already wound and squeezes out excess resin. Good fiber wet out is essential for removal of excess resin, which helps reduce resin rich areas and possible voids. Uncured resin parameters that are important

in the filament winding process are the resin viscosity and pot life. The mixed resin viscosity must be low enough that the moving tows may be impregnated yet high enough that the resin does not drip off the fiber tows. A viscosity level of 1-2 Pa-s or (1,000-2,000 cP) is preferred [8]. The pot life of the uncured resin is an important factor for tank produceability. Pot life should be long enough that large or complex structures can be wound without premature gelling or excessive exothermic reactions. The common defects found in filament wound parts are voids, delaminations, and fiber wrinkles.

Filament winding is an efficient process for manufacturing COPVs that takes advantage of the high strength of the fibers. Fuel storage tanks constructed of a composite overwrapped on a metal liner are used in many space, military, and commercial applications. The metal liner is used to prevent leakage associated with micocracks in the composite matrix. The liner also serves as the mandrel for the winding process. The winding process causes compressive stresses in the liner and tensile stresses in the composite [8]. When a thin-walled cylindrical pressure vessel is subjected to internal pressures a biaxial stress state is created. Stresses exist in both the axial and tangential directions the average tangential stress is given in Equation 1 and is valid regardless of the wall thickness [10]. In a closed thin-walled cylinder, Equation 2 approximates the axial stress developed.

$$\sigma_{hoop} = \frac{p \cdot d_i}{2 \cdot t} \tag{1}$$

$$\sigma_{axial} = \frac{p \cdot d_i}{4 \cdot t} \tag{2}$$

Where p is the internal pressure of the vessel d_i is the internal diameter of the vessel and t is the wall thickness of the vessel in question. The equations above are approximations for a thin-walled pressure vessel. A pressure vessel is generally considered thin-walled when the thickness of the vessel is about one-twentieth, or less, of its radius. Due to the biaxial stress state, the composite layup can be oriented to obtain the maximum desired performance.

2. Constitutive properties

Figure 2.3 fabricated COPV

A COPV structure is comprised of three or more constituents that form a unique third material as shown in Figure 2.3. The insoluble constituents of a COPV are combined on a macroscopic level and consist of the reinforcing fibers which are embedded in a polymer matrix [11]. Other constituents are coupling agents, coatings, and fillers. Coupling agents and coatings are applied to the fiber to improve wetting as

well as bonding with the matrix. They are used to improve the load transfer between the fiber and the matrix [8]. The mechanical properties of the new composite material are better than those of the parent materials. Composite materials are designed to exhibit the best properties of their constituents.

The manufacturing of a COPV starts with the incorporation of a large number of fibers into a thin layer of matrix to form a lamina or ply. Bonding plies on top of one another at various orientations creates a composite laminate, which is a flat or curved shell [12]. Fibers are the principal constituent and typically comprise a volume fraction of about 60%. Typically failure in a composite structure is fiber dominated, due to the preferred orientation of fibers in the direction of maximum loading. Although the fibers carry the primary load in the composite, the role of transferring the load to the fiber falls to the polymer matrix. The matrix is also responsible for binding the fibers and protecting them from the environment [13]. Because failure in COPVs is fiber dominated, the resin properties have typically been ignored in the literature. Studies have indicated that if all processing variables remain constant and resin properties are varied, the performance of the pressure vessel can vary as much as 20 – 35 percent [3]. There is little literature on the mechanics of how the polymer matrix influences the performance of filamentary structures or more specifically COPVs. During the 70's Garrett [14] did research on varying the failure strain of polyester in glass fiber cross-ply laminates. It was observed that at very low strain levels (0.4%) cracking occurred in the transverse plies [14]. In applications such as pressure vessels these transverse cracks are very undesirable and can lead to leakage. Laminates made from low failure strain (<4%) high

modulus resins exhibit catastrophic cracking. For lower modulus, higher strain-to-failure resins (~6%), the damage is spread in a controlled manner as the applied stress increases [2]. Therefore, a more flexible resin may extend the operational strain range of cross ply COPVs. Nahas [15] correlated that the stress required to cause significant matrix cracking is nearly equal to the yield strength of the matrix material. From a micromechanics approach of using the shear lag model, which assumes that at a fiber break shear stress in the matrix becomes very large while tensile stress at the fiber end goes to zero. Away from this area the shear in the matrix decreases while the load carried by the rest of the fiber increases [4]. Using the shear lag model, Rosen [16] hypothesized that an increase in matrix shear modulus (G) would lead to an increase in the strength of the composite.

Some resin dominated properties, such as interlaminar shear strength (ILSS), may influence the failure mode of filamentary structures [3]. Vessels with low ILSS tended to fail in the dome region. Conversely vessels with high ILSS (> 34 MPa) failed in the mid section as illustrated in Figure 2.4.

Figure 2.4 burst COPVs tested by Hypercomp Engineering Inc.

The fiber matrix bond strength is important to the transfer of load between the resin and the fiber. Some critical length of the fiber is necessary for the effective strengthening and stiffening of composite materials [13]. The resin properties investigated include: strain to failure (%ε), failure stress (σ_{ys}), and elastic modulus (E). Short beam shear tests are conducted to investigate the fiber matrix interaction [17]. The measured properties will be compared to actual tank burst pressures performed at ambient and liquid nitrogen temperatures. COPV performance will be evaluated by the performance efficiency rating (PER) which is defined by Equation 3 [3, 17].

$$PER = \frac{P \cdot V}{W} \quad (3)$$

Where:

P = pressure at burst

V = internal volume of the pressure vessel

W = the weight of the composite

CHAPTER III

MECHANICAL PROPERTIES OF POLYMERS

The word polymer is derived from the Greek words *polys* and *meros; Polys*, meaning numerous, and *meros*, meaning part. Structurally, polymers are long-chain molecules of very high molecular weight, often measured in the hundreds of thousands. For this reason, the term "macromolecules" is frequently used when referring to polymeric materials. Polymers can be classified in several manners. The synthesis method, molecular structure, or chemical family may classify polymers. However, for engineers the most convenient method to classify a polymer is by its temperature induced mechanical behavior. It is hoped that this research will help determine which classifications of polymers are suitable for using COPV and cryogenic conditions

Based on their thermal/mechanical behavior, polymers can be divided into three categories: thermosets, thermoplastics and elastomers. Polymers are composed of long three-dimensional molecular chains; the backbone of these chains is a string of carbon atoms. Although the three dimensional structure is very difficult to represent with a picture, Figure 3.1 provides a three-dimensional and two-dimensional representation of a linear polymer, polyethylene.

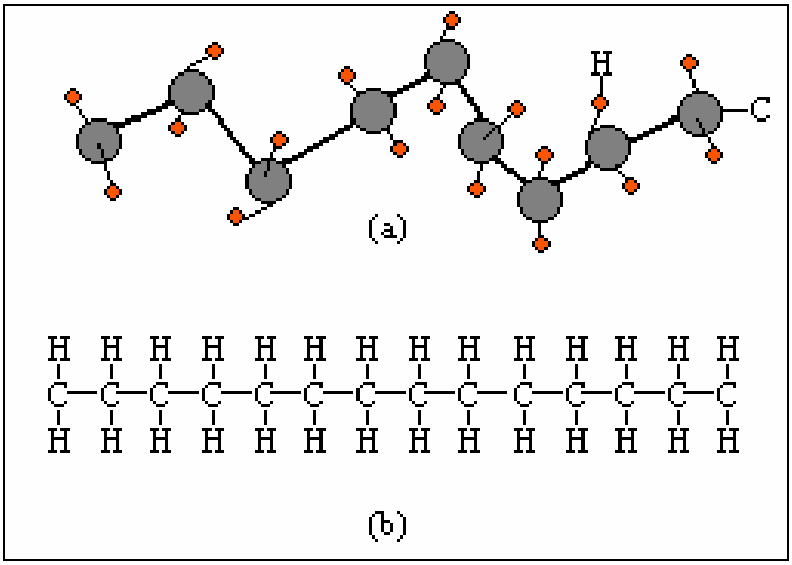

Figure 3.1 (a) three dimensional and (b) two dimensional representation of polyethylene

The difference between thermoplastics and thermosets is the degree of crosslinking. Crosslinking can be defined as strong covalent bonds joining the molecular chains that rigidly fix the molecules relative to each other. Thermoplastics are polymers whose molecular chains are not crosslinked. The molecular chains are joined only by Van Der Waals forces. Because there is no crosslinking in thermoplastics, there is no limit on the use of heating to reduce the viscosity to allow recycling into various shapes. Conversely, thermosets are heavily crosslinked, usually by an irreversible temperature treatment, and thus cannot be recycled into new shapes. Also, thermosets do not have a softening temperature; rather they degrade when a certain amount of heat is applied. Elastomers have an intermediate structure with some degree of crosslinking although they retain the ability to be recycled [18].

Polymers can also be classified according to their molecular structures: crystalline polymers, amorphous polymers, and semi-crystalline polymers. The basic molecular structures will be discussed in Section 3.1 followed by a discussion of the glass transition temperature phenomenon in the Glass Transition Section.

1. Crystalline polymers

Some polymers have a crystalline structure that displays both long-range and short-range order. Highly crystalline polymers are rigid, have a high melting temperature, and are more resistant to solvent penetration. Crystalline structure makes a polymer strong but also lowers its impact resistance. For example, samples of polyethylene prepared under high pressure (50 MPa) have high crystalline structures (95 - 99%), but are extremely brittle[19]. Because polymer molecules are long chains it might seem that they could not pack together regularly to form an ordered structure. However, research has shown that polymers may form lamellar (plate-like) crystals, as seen in Figure 3.2, with a thickness of 10 to 20 nm with parallel folded chains perpendicular to the face of the crystals[20]. The chains are on the order of approximately 100 carbon atoms long.

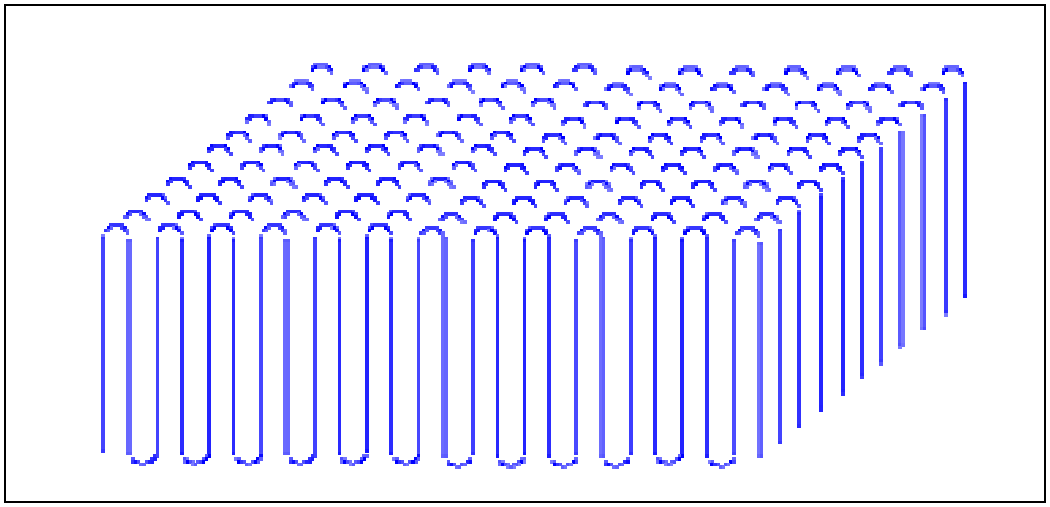

Figure 3.2 lamellar structure of a polymer crystal

2. Amorphous polymers

Polymer chains with branches, or irregular pendant groups, cannot pack together regularly to form crystals. Polymers without an ordered lamellar structure are called amorphous. A two-dimensional schematic of an amorphous polymer is shown in Figure 3.3. Amorphous regions of a polymer are made up of randomly coiled and entangled chains. Melting, which involves a large volume change, occurs in crystalline polymers when the ordered chains fall out of their crystal structures and become a disordered liquid. The glass transition is a change that occurs in amorphous polymers where there is negligible change in volume of the solid. Thermosets are a classic example of randomly oriented molecular chains.

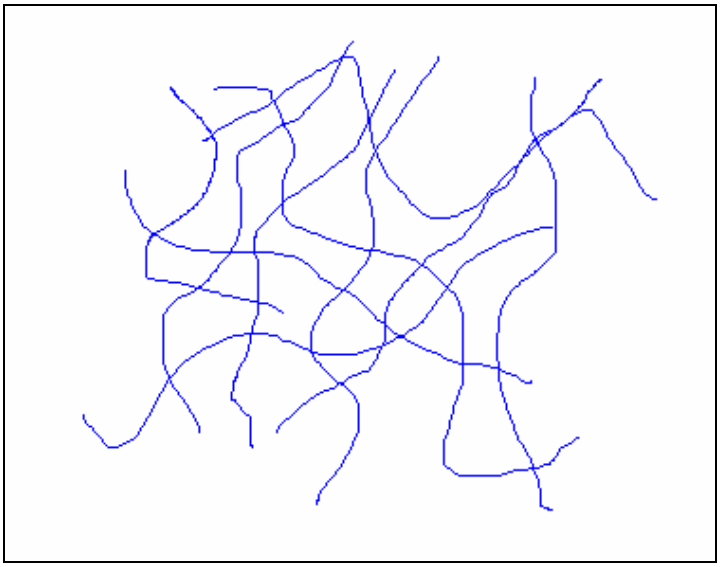

Figure 3.3 pictorial representation of random entangled polymer chains

3. Semi-crystalline polymers

Semi-crystalline polymers have both crystalline and amorphous regions. Semi-crystallinity is a desirable property for most plastics because they combine the strength of crystalline polymers with the flexibility of amorphous polymers. Semi-crystalline polymers are tough with an ability to bend without breaking. Semi-crystalline polymers have a melting temperature as well as a glass transition temperature.

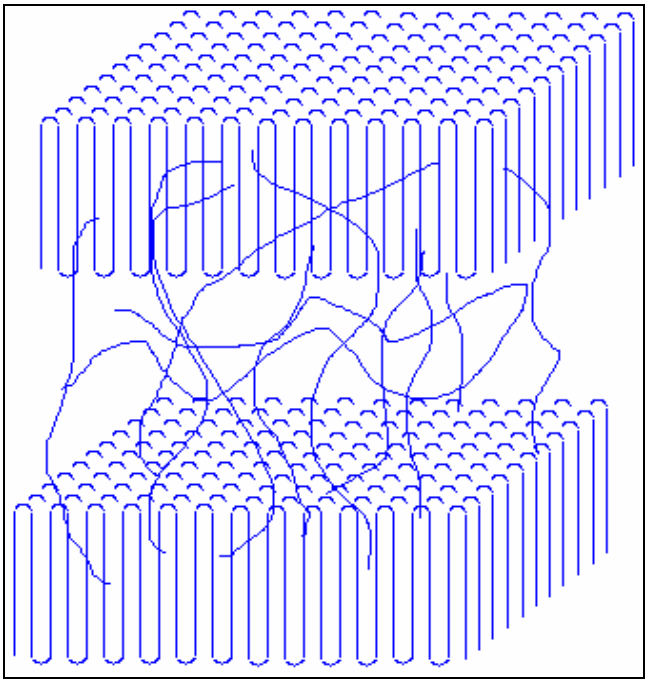

Figure 3.4 semi-crystalline structure

Figure 3.4 illustrates a semi-crystalline structure, with two distinct regions: the folded lamellar, or crystal portion, and the random amorphous region connecting the lamellar. The crystalline region only undergoes melting and the amorphous region only experiences the glass transition temperature. This is why the semi-crystalline polymer can have both a glass transition temperature and a melting temperature. Elastomers and thermoplastics are both examples of semi-crystalline polymers. Some elastomers and thermoplastics have set melting temperatures and also experience a glass transition temperature.

4. Stress-strain behavior of polymeric systems

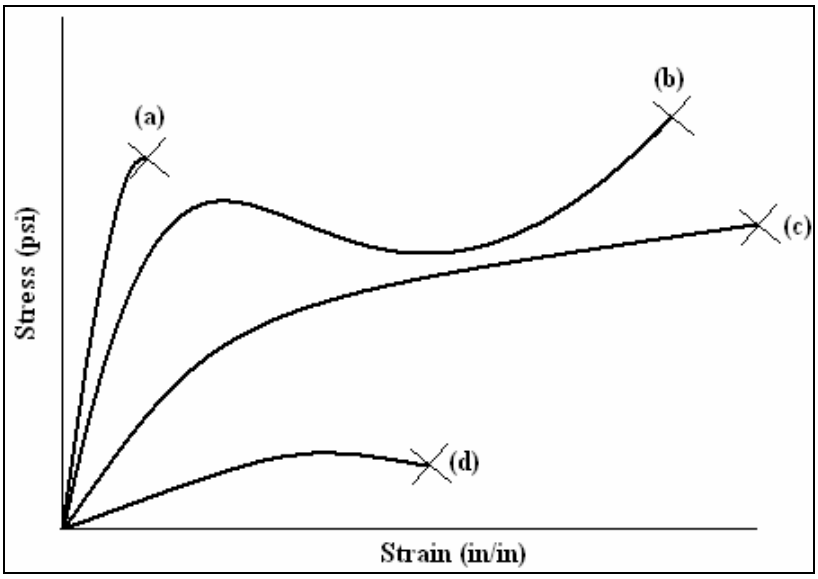

Figure 3.5 tensile behavior of polymers, (a)high-modulus, strong material with low toughness (b) high-modulus, strong, tough materials (c) low-modulus, strong, tough materials (d) low-modulus, weak materials, with low toughness

When polymers are strained in uniaxial tension they exhibit one of several general types of behavior as illustrated in Figure 3.5.

The time-dependent properties of polymers are referred to as viscoelastic properties [20]. For a comparative study, the time dependency of the polymers can be held constant for evaluation without rate effects.

The elastic modulus of a polymer is directly related to its intermolecular bonding. An applied stress will cause the molecular chains to move relative to one another as illustrated in Figure3.6.

If the intermolecular bonding is stiff and strong, the chains will resist the stress. As the chains move, some straining and rotation of the bonds will occur, these conformations will also aid in resisting the applied stress. Polymers with superior intermolecular bonding will also have the highest modulus [21].

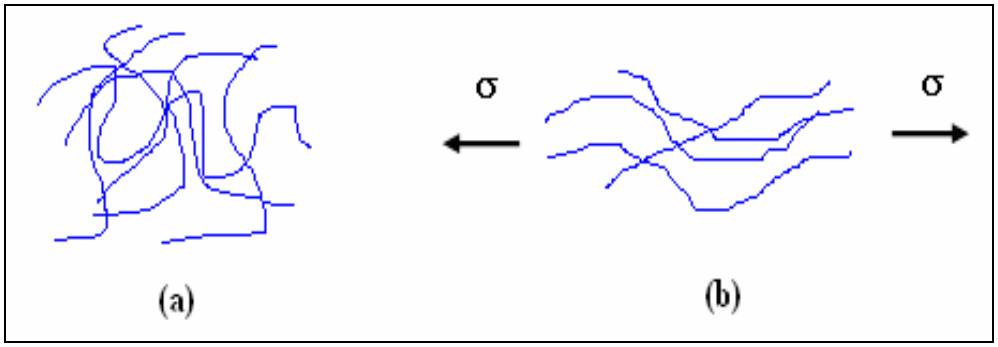

Figure 3.6 polymer chains (a) unstressed chains and (b) chains with an applied stress

As well as a time dependency, polymers are also sensitive to temperature. A change in temperature will cause dramatically different behaviors of similar polymers. Most notable is the difference in the stress strain response. Below a certain temperature, the glass transition temperature (T_g), polymers assume a rigid glassy structure. The tensile strength of the polymer increases while the strain to failure decreases. The remainder of this chapter will be discussing the phenomenon of T_g and the factors that affect this temperature.

5. The glass transition temperature

In a practical sense, the glass transition temperature of a polymer can be defined as the temperature, or narrow temperature range below which an amorphous polymer or

amorphous region is rigid and brittle and above which it is rubbery or viscous [21]. Qualitatively, the glass transition region can be interpreted as the onset of long range, coordinated molecular motion. While only one- to four-chain atoms are involved in motions below the glass transition temperatures, some ten- to 50-chain atoms attain sufficient thermal energy to move in the glass transition region [22]. Although the glass transition in polymers is not completely understood, there appears to be a correlation between the temperature and the flexibility of the molecules [21]. This idea can be illustrated by plotting the modulus of elasticity against the temperature of the polymer. When a polymer is stressed elastically in tension or compression, the chain ends are moved either apart or together respectively. Molecular motion depends on the presence of free volume[23]. For a polymer chain to change its conformation* the bonds must twist (torsion). The bonds are able to twist because of the tetrahedral structure of covalent bonds. This twist is a thermally activated process. At low temperatures there is not enough thermal energy to facilitate the twist, so the conformations become frozen. When the molecular chains are stressed the strain comes only from the extension of the covalent bonds.

* Conformation of a polymer molecule is the arrangement of the bond orientations

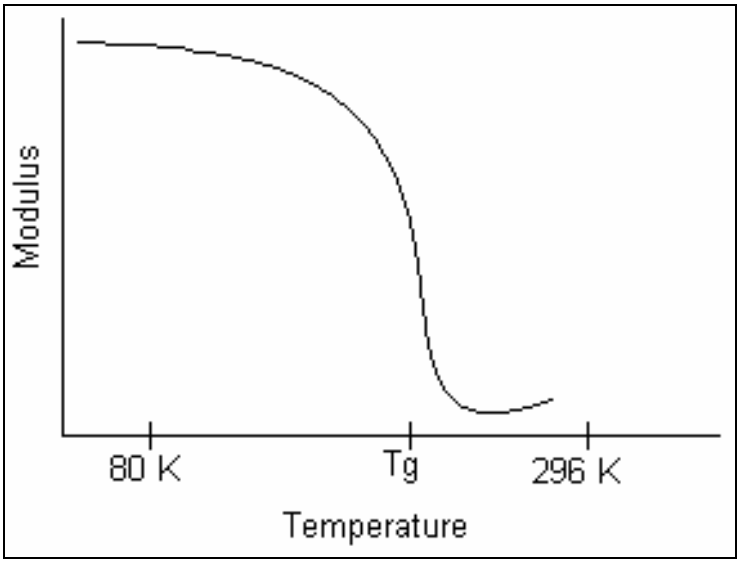

Figure 3.7 modulus versus temperature for a cross-linked polymer

Above the glass transition temperature the molecules are already in motion, so when the polymer is strained the molecules have no problem sliding over one another into a new position to relieve the applied stress. The exact temperature at which a polymer undergoes this change in mobility is heavily dependent on the structure of the polymer. Table 3.1 summarizes the glass transition temperature for some common polymers.

Table 3.1

T_g FOR COMMON POLYMERS

Polymer	Tg (°C)
Thermoplastic	
Polystyrene	125
Polyvinyl chloride	87
Polyethylene	-120
Thermoset	
977-3	120.4
Epon 828	30
Elastomer	
Silicone	-123
Polyisoprene	-73
Polybutadiene	-90

The factors that affect the glass transition temperature are chain flexibility, side groups, branching, cross-linking, and plasticizers. A polymer with a backbone that exhibits higher flexibility will have a lower Tg. This is because the activation energy for conformational changes is lower.

In a polymer whose backbone consist of carbon atoms, the presence of atoms or molecular groups different from hydrogen on the other two bonds has a great influence on the flexibility of the chain. That is, for the molecular segment to move to new positions, some rotation about the single bonds must occur. The degree to which the molecule can rotate about these bonds depends on the size of the side group and how much space the molecule requires [21]. If the molecule is small then the effect on the rotation will be minimal. So, if the side group is small there will be plenty of space for rotation and the Tg will also be low, but if the side group is large and hinders rotation, the

added stiffness will cause an increase in Tg. Figure 3.8 illustrates the addition of a side group (X) to a polyethylene backbone.

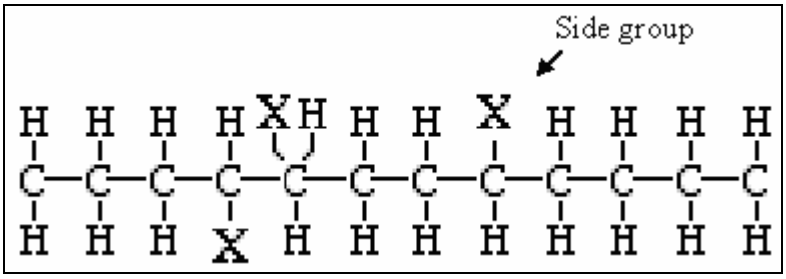

Figure 3.8 polyethylene backbone with side groups

Figure 3.9 illustrates branching that occurs when a side group attached to the main carbon backbone is removed and replaced with a linear chain with the same structure as the backbone.

Polymers with more branching have more chain ends, resulting in more free volume, which reduces T_g. However, the branches also hinder rotation, like large side groups, which increases T_g. Which effect is greater depends on the polymer in question, but T_g may increase or decrease.

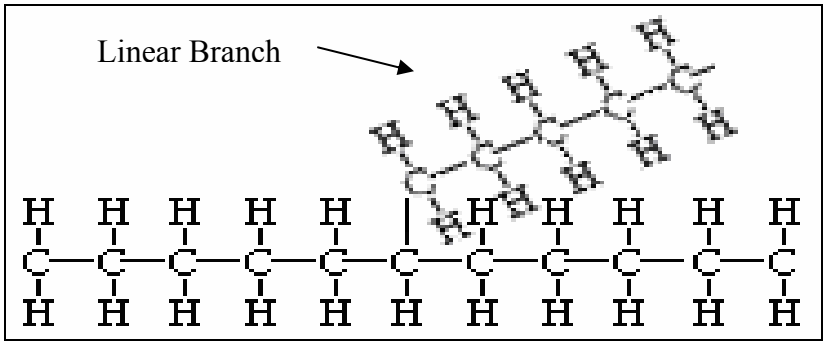

Figure 3.9 branching of polyethylene

A crosslink tightly bonds two molecular segments together and restricts their motion. As the cross linking density of the polymer increases, the restrictions on the back bone become wider spread and Tg increases [21]. If there are cross-links between the chains, they will be fixed relative to one another, making it impossible for them to slide past each other. Thermosets are heavily crosslinked, causing the molecular motion to be extremely restricted resulting in a high T_g.

The cross-linking in Figure 3.10 occurred by introducing sulfur atoms that either replace or rearrange the existing hydrogen atoms.

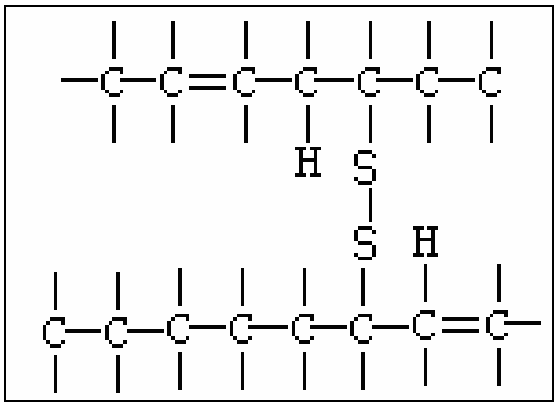

Figure 3.10 cross-linking of polyisoprene with sulfur

A plasticizer is a compound of relatively low molecular weight that is added to some polymers during processing. Plasticizers reduce the intermolecular bond strength by positioning themselves between the polymer molecules, separating them and lessening their interactions. This allows the polymer molecules to move more readily and the glass transition temperature to decrease[21].

The purpose of this section was to illustrate that resins have numerous types of chemical structures. The type of structure plays a major role in the performance of the material. Although complete microstructure characterization of the experimental resins is beyond the scope of this study, it will be needed in future work to completely understand the material systems.

CHAPTER IV

EXPERIMENTAL PROCEDURE

Use of CFRP tanks by the aerospace industry for storage of cryogenic fuels requires the resin to operate well below the T_g or in the brittle region as discussed in Chapter III. At these low temperatures, the mechanical properties of the matrix resins are dramatically different than at ambient temperature. To survive under these extreme conditions, various neat and modified resins are being investigated for cryogenic operation [24]. The material selection and subsequent, design and fabrication of the cryogenically-rated tanks must be able to accommodate both the mechanical loading strains and the thermal strains induced by the coefficient of thermal expansion (CTE) difference between the resin and fiber.

For industry to meet this application, a number of resins are being formulated for use in the fabrication of CFRP tanks for cryogenic fuel storage. However to down select the best candidates, a large number of variables, including material properties and manufacturing methods, must be evaluated. To reduce the number of variables associated with evaluating the various resin and fiber systems being developed, the approach at MSU is to test the resin and resin/fiber interface at LN_2 temperatures and correlate their properties with the actual burst test performance of cryogenic COPV storage tanks.

Although the materials will ultimately be used for storage of liquid hydrogen (LH_2 20K) and liquid oxygen (LOX 90K), the flammability of these liquids precludes usage at a university. For the initial screening tests, LN_2 will be used for safety reasons. NASA-MSFC has developed the capability to hydrostatically burst tanks with either LN_2 at steady state conditions. Linking the constitutive material behavior with cryogenic burst tank performance will provide a basis for down selection of viable material selection in the design of cryogenic COPVs.

A review of appropriate test methods for the evaluation of polymeric resins include tensile testing [25]. The short beam shear test [26] has been used as a qualitative method for evaluation of load transfer between the resin and fiber. although these methods are used for room temperature testing [3],their applicability to cryogenic testing will be evaluated.

1. Tensile testing

The standard test method for tensile testing of plastics is ASTM D 638-03 [25]. In this test a dog bone shaped specimen is loaded into a universal test machine, and the load required to elongate the specimen at a constant rate is recorded. The tensile test can be used to generate the stress-strain response of candidate resin systems. This standard applies to rigid polymer resins, such as PVC, whose glass transition temperature is above ambient temperature. Rigid polymers display a brittle, linear elastic stress vs strain response as shown in Figure 4.1. Published properties of polymeric resins include: elastic modulus (E), yield stress (σ_{ys}), ultimate stress (σ_{uts}), and toughness (K_{Ic}). All

tensile tests were conducted on a Model 5869 Instron 50 kN electro-mechanical load frame. A cryostat to hold a liquid nitrogen bath was constructed from a 37.8 liter container insulated with polyurethane foam and rigidly fixed to the load frame. Strain measurements were made with a cryogenically rated MTS extensometer.

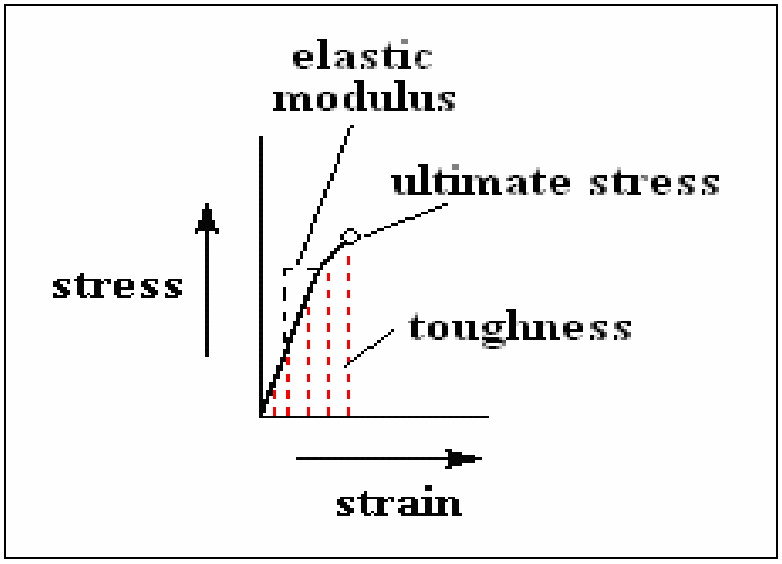

Figure 4.1 typical stress-strain curve for polymers at ambient temperatures

2. Tensile specimen geometry

Although ASTM D 638-03 provides recommendations for ambient temperature (273K) tensile tests of plastics, there is no standard for low-temperature tensile testing. A finite element analysis (FEA) study was performed to evaluate the dog bone geometry in the standard to ensure that the stress was distributed uniformly across the gage section as the response of the material was varied. The FEA software used was COSMOS [27]; a linear elastic model was assumed. Two-dimensional quadrilateral elements were used with an average aspect ratio of about 1.5. Linear elasticity was selected because of the

brittle nature of the polymer resins at liquid nitrogen temperatures. Large stresses are shown in red and low stresses are shown in blue. The results from the FE study of the ASTM dog bone are shown in Figure 4.2, which shows a stress riser at the transition from the tab to the gage section. Since the location of stress risers was the only thing of interest, any linear elastic material properties could be used. Because the properties of these resins at LN_2 temperature are unknown, an elastic modulus of 69 GPa and yield strength of 137 MPa were selected for the material properties. Boundary conditions for the specimen constrained one end, with the opposite end loaded in tension. Various transition geometries between the gauge section and the ends were investigated to minimize any potential stress concentrations. Figure 4.3 shows the final tensile geometry used for all the tests. The maximum stresses are located in the gage section.

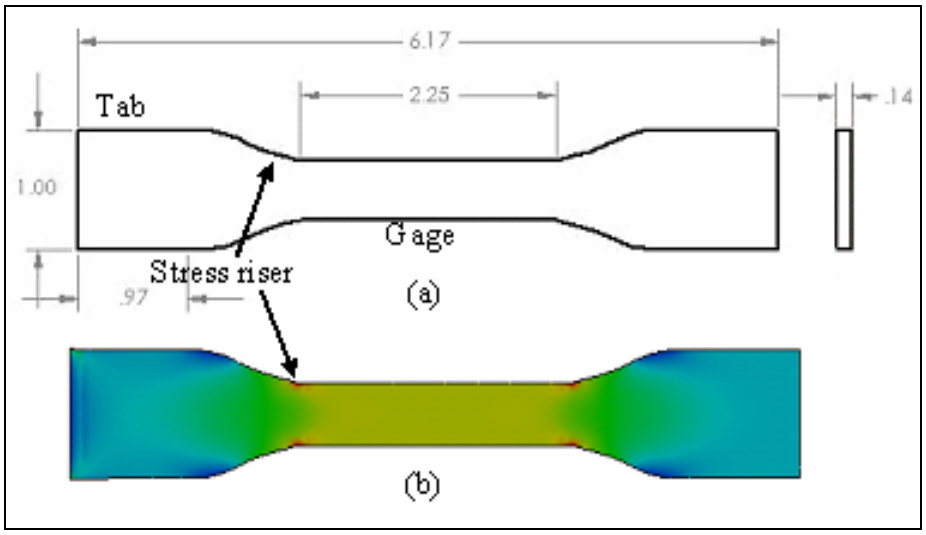

Figure 4.2 (a) standard ASTM D 638-91 dog bone (all dimensions are inches), (b) results of FEA showing stress concentration at the transition section.

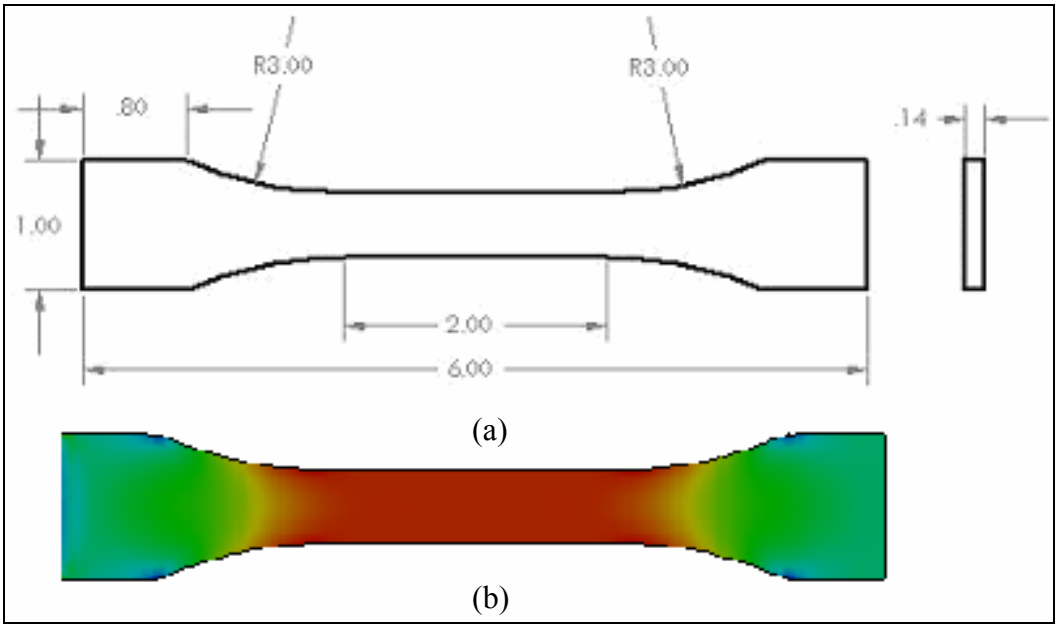

Figure 4.3 (a) modified dog bone geometry (b) results of FEA showing stress distributed over the gage section

Dog-bone shaped samples were cut from sheets of experimental resins that were supplied by NASA. The experimental resin systems were mixed thoroughly and out-gassed using a Rietschle type VCB-20 (02) vacuum pump to minimize bubbles. The out-gassed resin was then carefully poured into a two piece aluminum mold and cured for the desired amount of time in a BlueM model number EM-9665R1G-MPZ.GOP oven. The cured sheets of resin (305 mm x 203 mm x 3.5 mm) were removed from the aluminum mold and cut using a table top band saw with a diamond blade into (25 mm x 177 mm x 3.5 mm) strips, the strips were cut to the final shape shown in Figure 4.3 using a TensilKut model 10-33 specimen router table with a specialized jig.

3. Tensile test methodology

The test methodology of ASTM D 638 was followed using the modified specimen geometry shown in Figure 4.3. A total of five ambient and five liquid nitrogen tests were performed. After loading the specimen in the grips, the bolts on the grips were tightened with a torque wrench to 5.6 N-m. Next, the MTS model 634.11E-21 Axial extensometer, shown in Figure 4.4a, was attached to the specimen using rubber bands. The MTS extensometer has a reference gauge length of 25.4 mm and a -10% to +20% strain range. The specimen was then loaded into the cryostat, shown in Figure4.4b, and attached to the load frame operated in load control mode set at 0 N. The cryostat was filled with LN_2 and the specimen and grips were allowed to reach an equilibrium temperature of 77K. Prior to the start of the tensile test, the load frame control was transferred to extension control and the test was run at a constant cross head rate of 1.27 mm/min with load and extension data collected every 500 ms. After the test was completed the container was drained and the fractured specimen was removed.

(a) (b) (c)

Figure 4.4 (a) MTS extensometer mounted on specimen mounted in grips, (b) interior of cryostat, and (c) cryostat mounted on Instron load frame

Equation 4 and 5 are used to calculate the engineering stress and strain.

$$\sigma_e = \frac{F}{A} \tag{4}$$

$$\varepsilon_e = \frac{l_f - l_o}{l_o} \tag{5}$$

Where:
F = the load measured from the load cell

A = is the cross-sectional area of the specimen being tested

l_f = is the final gauge length

l_o = is the initial gauge length

However, strain (ε_e) is measured directly using the MTS extensometer.

4. Short beam shear test

The short beam shear test is used to determine the short beam shear strength of continuous fiber composites, which is used as a comparison method for composite materials [3]. The short beam shear strength is measured in accordance with ASTM D2344-00 [26]. Short beam shear specimens are made from the barrel section of a COPV. A statistically significant number of short beam shear samples can be machined from a single COPV. The standard uses Equation 6, which is the maximum shear stress of a homogeneous beam, to approximate the interlaminar shear strength (τ_{max}) of the composite.

$$\tau_{max} = \frac{3P}{4bh} \tag{6}$$

Where:

P = is the load recorded at failure

b = is the thickness of the specimen

h = is the height of the specimen

This equation predicts a parabolic shear stress distribution in the thickness direction. For homogeneous materials the maximum shear stress is located at the beams neutral axis. However, for composite materials the maximum shear stress may occur at some location where there are several stress interactions [8]. Although the interlaminar shear strength obtained from D 2344-00 is an approximation of the actual interlaminar shear strength, is useful for comparing different material systems. Various studies conducted at ambient temperature report that the larger the short beam shear strength the higher the burst

strength of the vessel [3, 17]. It remains to be seen if this phenomenon is applicable to cryogenic temperatures.

5. Short beam shear test methodology

Resin formulations for the composites were mixed according to manufacturers specifications using a Mettler PF11 682B scale. The resin was next applied by hand to the filaments using an EnTec model number 5K48W-180-4 filament winding machine; which wrapped the filaments around an aluminum 6061-T6 liners of 2 mm. thickness and 165 mm. outside diameter. The liner has a coat of Loctite Frekote® so that the composite may be easily removed from the liner. Figure 4.5 depicts pictorially the filament winding machine and mandrel used.

Figure 4.5 aluminum mandrel on filament winding machine

The winding of the filament consisted of 25 plies and then vacuum bagging of the mandrels using a Rietschle type VCB-20 (02) vacuum pump. The curing times varied for the different formulations using a BlueM model number EM-9665R1G-MPZ.GOP oven. The hoop wrapped composite was removed from the aluminum liner/mandrel. The composite hoop sections were cut into 12 mm thick strips using a band saw. These hoop sections were then cut into coupons with a Buehler SampLmet 2 Abrasive Cutter. The edges of the sample were polished for approximately 30 s with a 400 grit disc to eliminate the machining marks. Final specimen thickness ranged from 3.4 mm to 4.2 mm as seen in Figure 4.6 depending on the fiber resin system used.

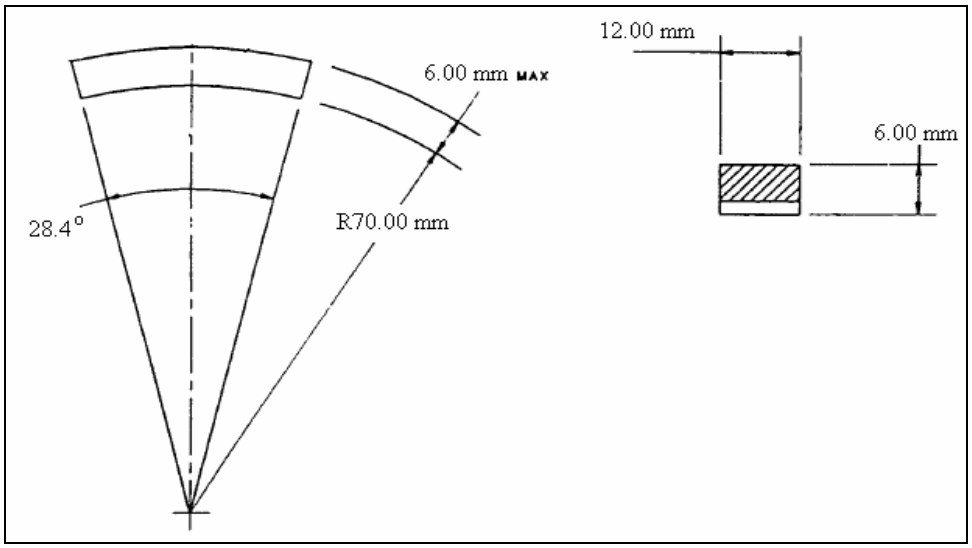

Figure 4.6 ASTM D2344-00 curved specimen configuration for short beam shear specimens (dimensions are in inches)

A total of five ambient and five LN_2 tests were performed per resin formulation. Tests were conducted on a Model 5869 Instron 35 kN electro-mechanical load frame at a constant rate of 1.27 mm/min. A cryostat to hold a liquid nitrogen bath was constructed from a block of aluminum insulated with polyurethane foam and rigidly fixed to the load frame. Figure 4.7 illustrates the specimen fixture assembly. Figure 4.8 shows a schematic of the specimen assembly that was used for this study.

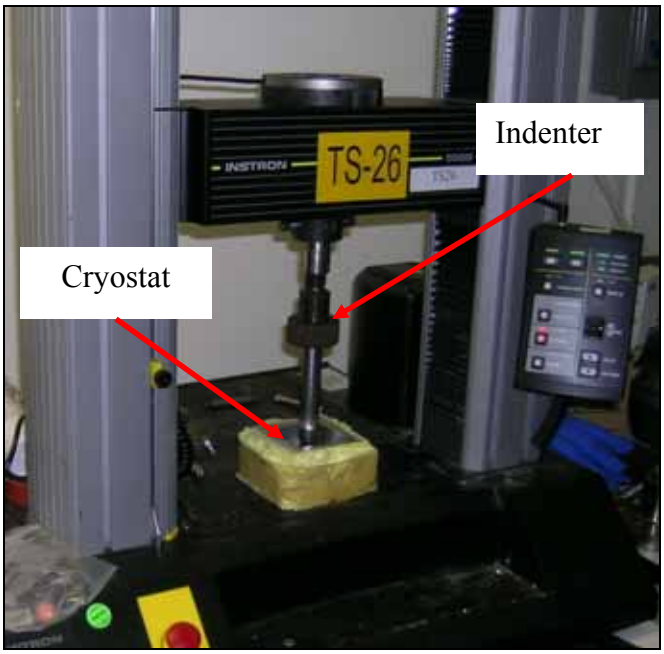

Figure 4.7 short beam shear fixture

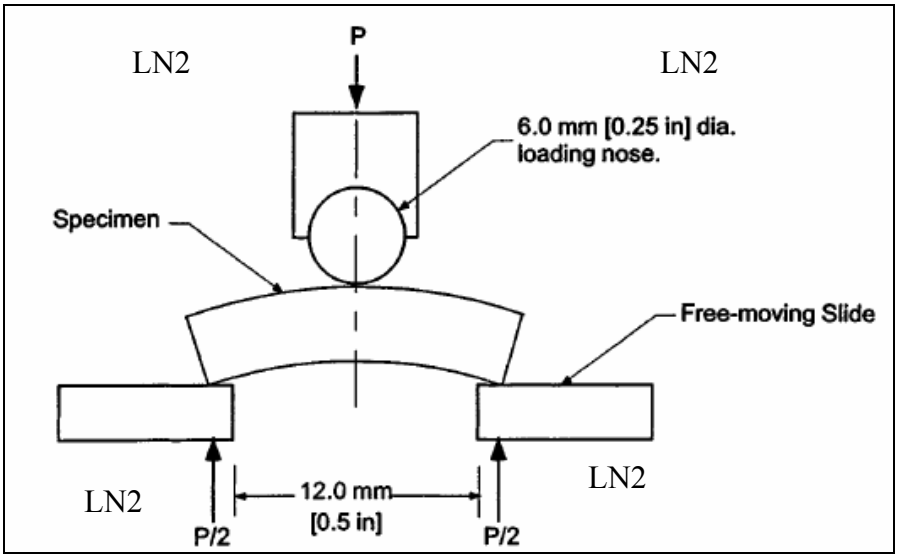

Figure 4.8 ASTM D2344-00 test configuration for short beam shear test of composite laminates

The specimen assembly was submerged in liquid nitrogen for 5 min to ensure that the specimen was at a stable temperature prior to testing. Termination of the test was due to either: a 25% decrease in loading or the displacement of the cross head is greater than the thickness of the specimen. After the test was completed, the specimen was removed from the nitrogen bath and the failure load and mode were recorded [26].

6. COPV tank fabrication

Based on the resin system under evaluation, the COPVs were fabricated by wet winding. The resin was applied to the filaments using an EnTec model number 5K48W-180-4 filament winding system as seen in Figure 4.6. All tanks were fabricated by wrapping around undressed aluminum mandrels. Tension was set to 26.6 N and monitored for all winding. A different winding sequence was used for the COPVs that

supported the short beam shear test specimens than was used in the COPV burst test specimens. The filament winding for short beam shear test specimens consisted of 25 hoop wraps. One vessel was made for each combination of short beam shear specimens. Seven each COPVs fabricated for the burst tests were wound using 5 hoop and 2 (+18º/-18º) helical wraps. After winding, all COPVs were cured with standard or manufactured recommended cure cycles as appropriate to the individual systems using a BlueM model number EM-9665R1G-MPZ.GOP oven.

7. Liquid nitrogen pressure testing

This procedure defines the test requirement to burst test cryogenic capable COPV's to ensure that the fabricated vessels meet or exceed the design requirements. The vessels that were investigated in this study are listed in Table 4.1. A standard carbon fiber tow, M30SC-18K, was used in the fabrication of all the COPVs. The only commercially available resin evaluated was the EPON™ 862/W resin system. The TD-111103 and UR 469 are experimental resins that are proprietary to the NASA.

Table 4.1

COPV TANK CONFIGURATIONS

Tank No.	Resin System	Fiber System	COPVs	Short Beam Shear Tanks.
A	EPON™ 862/W	Toray M30SC-18K	7	1
B	TD 111103	Toray M30SC-18K	7	1
C	UR 469	Toray M30SC-18K	7	1

The resin and fiber systems being developed at the NASA are more flexible at colder temperatures and offer the potential for high strength cryogenic vessels. Figure 4.9 is a schematic of the NASA test facility. In these tests, the COPVs will be filled using a high pressure (137 MPa) tank downstream of the COPV, and an insulated bath with liquid nitrogen (LN2). Then the high-pressure (137 MPa) tank is pressurized with gaseous helium (GHe), forcing LN_2 from the high pressure tank into the COPV and thereby pressurizing the COPV with LN_2. The pressure is slowly increased until the COPV fails. Ambient temperature hydrostatic tests on each of these resin/fiber systems have been conducted to ensure that the strength of the system is known. The tests record tank temperature, pressure, and strain in the outer fiber. These tests are performed in a secluded test area to ensure that the rupturing vessel does not cause injury or damage.

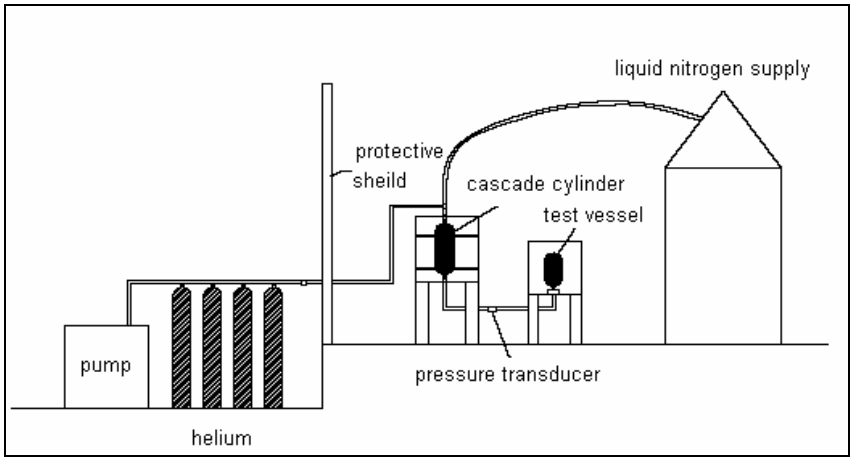

Figure 4.9 cryogenic burst test set-up

The COPV, high-pressure (137 MPa) tank, and bath will be filled with LN_2 from the supplied Dewar, through two hand-operated valves, vacuum jacketed flex hose and

high-pressure tubing. A large remote-operated valve (ROV) connected to a dewar will be opened to begin filling a bath surrounding the test vessel. Once the bath is filled to a level above the COPV, a smaller ROV will be opened to fill the COPV and high pressure tank. The operators will clear the area. Once clear, the remote-operated valve that allows fluid into the bath will also be closed. The solenoid valves to control the pump and allow the flow of GHe will be opened, increasing pressure on the high-pressure tank. This pressure will force LN_2 from the high-pressure tank into the COPV, thereby pressurizing the COPV with LN_2. Pressure in the tank shall be increased until the tank reaches the burst pressure. A relief valve is provided to ensure that the mechanical and instrumentation items do not see pressure above their rated value of 12,000 psig. Solenoid valves are provided to power the ROV and use GHe to provide pressure to the valves. Should the GHe supply be depleted ROV-5 will open relieving pressure on the vessel, and the SOV's will close eliminating further pressurization.

The liquid nitrogen burst testing was performed by NASA-Marshall Space Flight Center personnel. The method for the burst testing was obtained from the technicians responsible for testing the vessels.

CHAPTER V

RESULTS AND DISCUSSION

Table 5.1 lists the properties obtained from the neat resin testing. Table 5.2 lists the short beam shear testing and Table 5.3 lists the actual burst test data. The tests were conducted according to the procedures discussed in Chapter IV. After the tests were complete the raw data was imported into a data reduction software and analyzed. Due to the complexity and cost of testing only one data point is currently available for the LN_2 tank burst test. Seven bottles of each material type are available for further testing, so that a statistically meaningful data set can be established.

Table 5.1

NEAT RESIN PROPERTIES

	Ambient Temperature (295K)			**Liquid Nitrogen (77K)**		
Resin System	**E (MPa)**	**UTS (MPa)**	**%ε**	**E (MPa)**	**UTS (MPa)**	**%ε**
TD 111103*	503 ± 27	11 ± 3	180 ± 2	6143 ± 262	151 ± 21	2.4 ± 0.43
EPON™ 862/W*	2647 ± 144	77 ± 8	5 ± 1	6749 ± 406	133 ± 14	1.9 ± 0.41
UR 469**	10	2	50	5502	117	2.31

* five samples per temperature condition

** one data point avaliable

The neat resin properties in Table 5.1 illustrate the difference between ambient and LN_2 performance. TD 111103 is a thermoset epoxy resin, EPON™ 862/W is also a thermoset epoxy resin that is heavily crosslinked, and UR 469 is a thermoset polyurethane resin. At ambient conditions the TD 111103 resin was ductile, as evidenced by the $\varepsilon_f \approx 180\%$ and low UTS. While the EPON™ 862/W thermoset epoxy resin has a much lower strain to failure and larger UTS. The thermoset polyurethane system was extremely rubbery at ambient conditions with a modulus of 10 MPa and failure strength of 2 MPa.

At 77K the modulus and UTS of all three systems increased while conversely the strain-to-failure decreased. At 77K the polymer chains do not have sufficient thermal energy to freely rotate causing the extension to decrease and the strength to increase. This dramatic change in performance is related to the chemical structure of the polymer. The two epoxies and the polyurethane have amorphous structures with varying amounts of crosslinking.

Table 5.2

SHORT BEAM SHEAR TEST RESULTS

Tank Resin System	**Tank Fiber System**	**295K SBSS (GPa)**	**295K failure mode**	**77K SBSS (GPa)**	**77K failure mode**
TD 111103	M30SC-18K	11 ± 0.5	inelastic deformation	45 ± 4	interlaminar shear
EPON™ 862/W	M30SC-18K	29 ± 1.0	interlaminar shear	36 ± 3	interlaminar shear
UR 469	M30SC-18K	7 ± 0.6	inelastic deformation	62 ± 3	interlaminar shear

Table 5.2 summarizes the short beam shear tests which were conducted to evaluate the resin/fiber interface. At 295K the failure mode of the three systems differed, but when tested at 77K the failure modes were the same. The two NASA experimental resins displayed higher SBSS values than the commercially available EPON™ 862/W system

Table 5.3

PRESSURE VESSEL BURST DATA

Tank Resin System	**Tank Fiber System**	**295K - H_2O Burst Pressure (MPa)**	**295K - H_2O P.E.R. (x 10^6 cm)**	**77K-LN_2 Burst Pressure (MPa)**	**77K-LN_2 P.E.R. (x 10^6 cm)**
Bare Al liner**	N/A	8.9	NA	11.4	NA
Dry fiber**	M30SC-18K	41.1	5.27	43.4	5.56
TD 111103**	M30SC-18K	46.7	4.90	54.2	5.68
EPON™ 862/W**	M30SC-18K	52.6	5.47	35.8	3.72
UR 469**	M30SC-18K	42.4	4.61	54.9	5.98

Table 5.3 summarizes the COPV burst data. The burst vessels failed in the mid section as expected from Equation 1, which predicts the largest stresses in the hoop or mid section. Due to the time and cost of testing only one data point is currently available, but more testing is scheduled as funding permits.

CHAPTER VI

CONCLUSIONS AND FUTURE WORK

The resin and resin/fiber interface have been evaluated in addition to COPV burst tests. Testing of neat resin and resin/fiber composite coupons were conducted to establish a statistically meaningful data base of mechanical properties at LN_2 temperatures. While this data remains to be comprehensively correlated with the COPV performance at LN_2 temperatures, certain trends can be mentioned. It appears that if a matrix with a failure strain of greater than 2% can be achieved, then the performance of the COPV will be superior to identical COPVs manufactured with a less ductile resin.

The characteristics of the fiber/matrix interface play a major role in the mechanical behavior of the composite. The prime role of the interface is to transfer stress from the matrix to the fiber, and the ability of the stress transfer is defined as the interfacial shear strength (IFSS) [28]. This quantity is a measure of how well the composite will perform. Composites with a high IFSS can be expected to have superior performance compared to those with a lower IFSS. The IFSS is a composite property that needs to be examined. The quality of the fiber matrix interface at low temperatures could explain the increase in performance of certain fiber/resin combinations. Ultimately no solid trends can be observed with only one data point. Seven COPVs of each material type have been made and ready for testing.

If the performance of the individual constituents can be correlated with the ultimate tank performance, then a methodology for material selection in the design of COPV cryogenic storage tanks can be established. The trends that have been observed seem to hold true but more testing needs to be done so that a statistically meaningful database may be compiled. Also, the chemical composition of the materials needs to be understood so that the materials may be fully characterized. Perhaps the change in behavior from ambient to LN_2 may be explained by understanding what changes are taking place on a molecular level.

Future studies will need to address the issues of thermal shock and cycling that the materials will be subjected. This work has laid the foundation for a method to quickly and efficiently screen candidate material systems for COPV fabrication.

REFERENCES CITED

1. Sloop, J.L., *Liquid Hydrogen as a Propulsion Fuel, 1945-1959*. The NASA history series. 2004: Scientific and Technical Information Office 1978 NATIONAL AERONAUTICS AND SPACE ADMINISTRATION.

2. K. W. Garrett, J.E.B., *The Effect of Resin Failure Strain on the Tensile Properties of Glass Fiber-Reinforced Polyester Cross-Ply Laminates.* Journal of Materials Science, 1977. 12: p. 2189-2194.

3. T. J. Lu, X.J., X. R. Gu, *The Effect of Resin Properties on the Strength of Filamentary Structures.* Journal of Strain Analysis, 1989. 24(2): p. 107-113.

4. D. Cohen, K.L., *The Influence of Epoxy Matrix Properties on Delivered Fiber Strength in Filament Wound Composite Pressure Vessels.* Journal of Reinforced Plastics and Composites, 1991. 10: p. 112-131.

5. Kim, T.D. *Fabrication of a Thin Unlined Reusable Filament Wound Composite Cryogenic Tank*. in *7th Japan International SAMPE*. 2001. Tokyo.

6. Addax. *Basic Filament Winding Process*. 2005 [cited; Available from: www.addax.com/technology/filament_winding.html.

7. Strong, A.B., *Fundamentals of Composites Manufacturing: Materials, Methods, and Applications*. 1 ed. 1989, Dearborn: Society of Manufacturing Engineers.

8. Mallick, P.K., *Fiber Reinforced Composites*. 1993, New York: Marcel Dekker, Inc.

9. Tsai, S.W., *Composite Design*. 1987, Dayton OH.

10. Shigley, J. and C. Mischke, *Mechanical Engineering Design*. 6 ed. 2001, New York: McGraw-Hill.

11. Kaw, A.K., *Mechanics of Composite Materials*. 1997, Boca Raton: CRC Press LLC.

12. Jones, R.M., *Mechanics of Composite Materials*. 2nd ed. 1999, Philadelphia: Taylor & Francis.

13. Callister, W.D., *Materials Science and Engineering An Introduction*. Fifth Edition ed. 1999: John Wiley & Sons, Inc.

14. K. W. Garrett, J.E.B., *Multiple transverse fracture in 90 degree cross-ply laminates of a glass fibre-reinforced polyester.* Journal of Materials Science, 1977. 12: p. 157-168.

15. Nahas, M.N., Composites, 1985. 16: p. 148.

16. Rosen, W.B., *Tensile Failure of Fibrous Composites.* AIAA Journal, 1964. **2**(11): p. 1985-1991.

17. Xing, J., *Composites and Micromechanics: Influence of Matrix on the Strength of Filamentary Pressure Vessels*, in *The First Pacific Rim International Conference on Advanced Materials and Processing (PRICM-1)*. 1992, The Minerals, Metals & Materials Society.

18. Askeland, D.R., *The Science and Engineering of Materials*. 3rd ed. 1994, Boston: PWS Publishing Company.

19. Kaufman, S.H., *Introduction to Polymer Science and Technology*. 1997, New York: Wiley

20. Carrahen, C.E., *Polymer Chemistry: An Introduction*. 4th ed. 1996, New York: Marcel Dekke.

21. G. R. Moore, D.E.K., *Properties and Processing of Polymers for Engineers*. 1984, Englewood Cliffs: Prentice-Hall, INC. 209.

22. Sperling, L.H., *Physical Polymer Science*. 3rd ed. 2001, New York: Wiley.

23. Eyring, H., J. Chem. Phys, 1936. 4: p. 283

24. Khian-Heng, J., *Alternative Carbon Fiber Reinforced Polymer (CFRP) Composites for Cryogenic Applications*, in *Mechanical Engineering Department*. 2004, Mississippi State University: Starkville.

25. ASTM, *Standard Test Method for Tensile Properties of Plastics*. 2003. p. 15.

26. ASTM, *Standard Test Method for Short-Beam Strength of Polymer Matrix Composite Materials and Their Laminates.* 2000. D 2344 / D 2344M-00.

27. *COSMOS*. 2004, Structural Research and Analysis corporation. p. Finite Element Analysis Software.

28. Zhou, *Interfacial Properties of Polymer Composites Measured by Push-out and Fragmentation Tests.* Composites: Part A applied science and manufacturing, 2001. 32: p. 1543-1551.